

Carrier and magnetism engineering for monolayer SnS_2 by high throughput first-principles calculations

Qing Zhan(詹庆), Xiaoguang Luo(罗小光), Hao Zhang(张皓), Zhenxiao Zhang(张振霄), Dongdong Liu(刘冬冬), and Yingchun Cheng(程迎春)

Citation: Chin. Phys. B, 2021, 30 (**11**): 117105. DOI: 10.1088/1674-1056/ac2805
Journal homepage: http://cpb.iphy.ac.cn; http://iopscience.iop.org/cpb

What follows is a list of articles you may be interested in

Carrier and magnetism engineering for monolayer SnS_2 by high throughput first-principles calculations

Qing Zhan(詹庆), Xiaoguang Luo(罗小光), Hao Zhang(张皓), Zhenxiao Zhang(张振霄), Dongdong Liu(刘冬冬), and Yingchun Cheng(程迎春)
Chin. Phys. B, 2021, 30 (**11**): 117105. DOI: 10.1088/1674-1056/ac2805

Anisotropic thermoelectric transport properties in polycrystalline $SnSe_2$

Caiyun Li(李彩云), Wenke He(何文科), Dongyang Wang(王东洋), and Li-Dong Zhao(赵立东)
Chin. Phys. B, 2021, 30 (**6**): 067101. DOI: 10.1088/1674-1056/abeee1

First-principles investigation of the valley and electrical properties of carbon-doped α-graphyne-like BN sheet

Bo Chen(陈波), Xiang-Qian Li(李向前), Lin Xue(薛林), Yan Han(韩燕), Zhi Yang(杨致), and Long-Long Zhang(张龙龙)
Chin. Phys. B, 2021, 30 (**5**): 057101. DOI: 10.1088/1674-1056/abddac

First-principles calculations of F-, Cl-, and N-related defects of amorphous SiO_2 and their impacts on carrier trapping and proton release

Xin Gao(高鑫), Yunliang Yue(乐云亮), Yang Liu(刘杨), and Xu Zuo(左旭)
Chin. Phys. B, 2021, 30 (**4**): 047104. DOI: 10.1088/1674-1056/abe3f7

Strain and interfacial engineering to accelerate hydrogen evolution reaction of two-dimensional phosphorus carbide

Tao Huang(黄韬), Yuan Si(思源), Hong-Yu Wu(吴宏宇), Li-Xin Xia(夏立新), Yu Lan(蓝郁), Wei-Qing Huang(黄维清), Wang-Yu Hu(胡望宇), and Gui-Fang Huang(黄桂芳)
Chin. Phys. B, 2021, 30 (**2**): 027101. DOI: 10.1088/1674-1056/abbbe7

SPECIAL TOPIC — Two-dimensional magnetic materials and devices

Carrier and magnetism engineering for monolayer SnS_2 by high throughput first-principles calculations*

Qing Zhan(詹庆)[1,†], Xiaoguang Luo(罗小光)[2,†], Hao Zhang(张皓)[1], Zhenxiao Zhang(张振霄)[1], Dongdong Liu(刘冬冬)[1], and Yingchun Cheng(程迎春)[1,‡]

[1] *Key Laboratory of Flexible Electronics & Institute of Advanced Materials, Jiangsu National Synergetic Innovation Center for Advanced Materials, Nanjing Tech University, Nanjing* 211816, *China*

[2] *Frontiers Science Center for Flexible Electronics (FSCFE), Shaanxi Institute of Flexible Electronics (SIFE) & Shaanxi Institute of Biomedical Materials and Engineering (SIBME), Northwestern Polytechnical University (NPU), Xi'an* 710129, *China*

(Received 30 April 2021; revised manuscript received 15 September 2021; accepted manuscript online 18 September 2021)

Two-dimensional (2D) semiconducting tin disulfide (SnS_2) has been widely used for optoelectronic applications. To functionalize SnS_2 for extending its application, we investigate the stability, electronic and magnetic properties of substitutional doping by high throughput first-principles calculations. There are a lot of elements that can be doped in monolayer SnS_2. Nonmetal in group A can introduce p-type and n-type carriers, while most metals in group A can only lead to p-type doping. Not only 3d, but also 4d and 5d transition metals in groups VB to VIIIB9 can introduce magnetism in SnS_2, which is potentially applicable for spintronics. This study provides a comprehensive view of functionalization of SnS_2 by substitutional doping, which will guide further experimental realization.

Keywords: SnS_2, high throughput first-principles calculations, carrier, magnetism

PACS: 71.15.Mb, 74.62.Dh **DOI:** 10.1088/1674-1056/ac2805

1. Introduction

Tin disulfide (SnS_2) is van der Waals semiconductor with an indirect band gap of 1.58 eV.[1] Free-standing SnS_2 monolayer can be prepared by mechanical exfoliation,[2] liquid exfoliation,[3] as well as chemical vapor deposition. SnS_2 has been demonstrated for various applications such as solar cells,[4] field-effect transistors,[5] lithium-ion batteries,[6] photothermal therapeutics,[7] catalysis and sensors.[8,9] To extend its application, chemical doping has been proposed experimentally and theoretically as an effective strategy.[10–14] For example, SnS_2 monolayer doped with Fe has been verified as a two-dimensional (2D) dilute magnetic semiconductor.[15–17] Till now various chemical doping, such as Li, B, C, N,O, F, Na, Mg, Al, P, Cl, K, Ca, Ti, V, Cr, Mn, Fe, Co, Ni, Cu, Zn, Ga, As, Se , Br, Sr, Y, Zr, Nb, Mo, Tc, Ru ,Rh, Pd, Ag, Cd, In, Sn, Te, I, W, Re, Os, Ir, Pt, Au and Hg have been investigated by first-principles calculations.[1,18–23] However, there are some other elements doping absent, such as Be, Si, S, Sc, Ge, Rb, Sb, Ba, Lu, Hf, Ta, Tl, Pb, Bi, Po, At, Fr and Ra. In addition, debates remain. For example, Li and Na doped SnS_2 is predicted to be magnetic,[24] which is different from nonmagnetic results.[18] Therefore, a comprehensive investigation of chemical doping in SnS_2 is necessary.[25]

In this paper, we systematically investigate the stability, electronic structure and magnetic properties of monolayers SnS_2 doped with foreign elements, based on high-throughput first-principles calculations. We firstly screen out the elements which can be effectively doped in SnS_2 with high stability. Then the effect of dopants on carrier in SnS_2 is discussed. More importantly, we find that monolayer SnS_2 systems doped with elements in VIB, VIIB, VIIIB8, and VIIIB9 groups show large binding energies with non-zero magnetic moment, indicating high possibility of fabrication experimentally and application in spintronics. Our present work provides a comprehensive view regarding chemical doping in SnS_2 and that predicts chemical doping is an effective strategy to functionalize SnS_2 for various applications, such as field effect transistor, optoelectronic device and spintronic technology.

2. Computational details

First-principles calculations are carried out by using the projector-augmented wave method implemented in the Vienna *ab initio* simulation package (VASP) based on density functional theory.[26] The Perdew–Burke–Ernzerhof (PBE) functional of the generalized gradient approximation (GGA) is adopted for electron exchange and correlation interactions.[27,28] The van der Waals interactions between layers are corrected using the DFT-D3 functional. The kinetic energy cut-off of the wave function is set to 500 eV. To mimic the defects in monolayer SnS_2, a $4 \times 4 \times 1$ supercell is used and a $4 \times 4 \times 1$ k-mesh sampling is applied. The ions relaxation is achieved until the force for per atom is less than 0.01 eV/Å and the total energy converges to 10^{-5} eV. A vacuum spacing of 20 Å is used to prevent interaction between adjacent slabs.

*Project supported by the National Natural Science Foundation of China (Grant No. 91833302).

†These authors contributed equally.

‡Corresponding author. E-mail: iamyccheng@njtech.edu.cn

© 2021 Chinese Physical Society and IOP Publishing Ltd

3. Results and discussion

3.1. Structural properties and binding energies

Pristine monolayer SnS_2 is hexagonal with space group D_{3d} ($P\bar{3}m1$). The optimized lattice constants of the $4\times4\times1$ supercell are $a=b=14.80$ Å. When removing one Sn/S atom from the monolayer SnS_2 supercell, a V_{Sn}/V_S will be created with corresponding vacancy concentration of 6.25%/3.125%. Figure 1 shows the structure of a $4\times4\times1$ SnS_2 supercell doped by X_{Sn} and X_S.

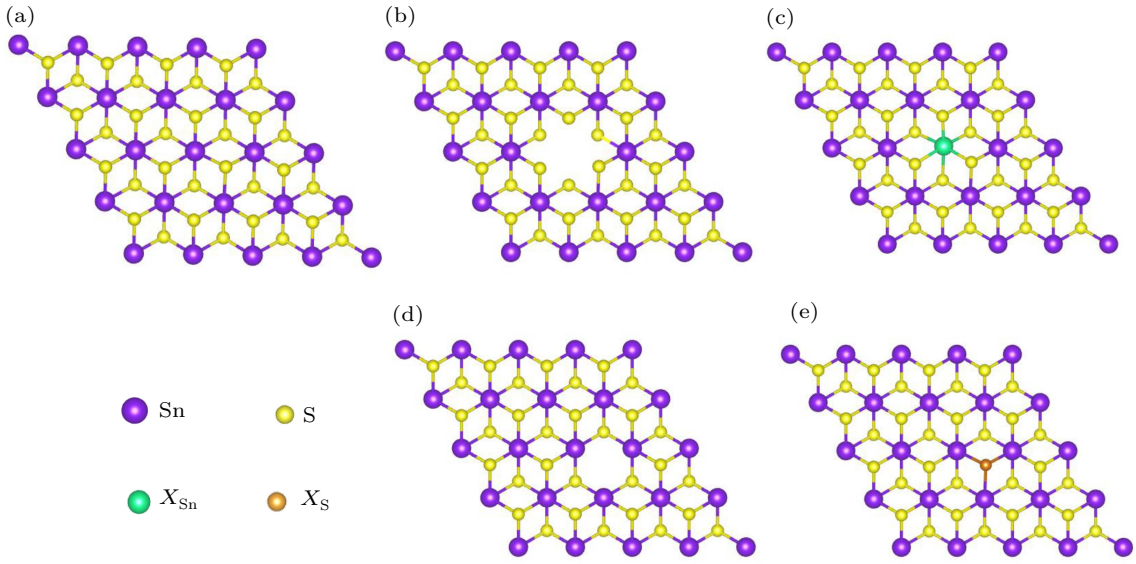


Fig. 1. Top view of the relaxed structures for (a) pristine, (b) Sn-vacant monolayer SnS_2, (c) single X_{Sn} doped monolayer SnS_2, (d) S-vacant monolayer SnS_2, (e) single X_S doped monolayer SnS_2 (X_{Sn} and X_S indicate Sn and S substitutions). The purple, yellow, green and orange balls denote the Sn, S, X_{Sn} and X_S atoms, respectively.

3.2. Binding energy

To check the stability of different dopants, we calculated the binding energies for various doping systems, as summarized in Fig. 2. The binding energy E_b is defined as $E_b = E_v + \mu - E_d$, where E_v is the energy of a relaxed SnS_2 monolayer with one Sn/S vacancy, μ is the energy of the doped atom, and E_d is the energy of a relaxed SnS_2 monolayer with one Sn/S atom replaced by a X_{Sn}/X_S atom.

Figure 2(a) shows the binding energy of main group metal doped in SnS_2. Only the binding energy of Al and Si is higher than that of Sn, indicating Al and Si are energetically favorable doped in SnS_2. The binding energies of Be, Ca, Sr, Ba, Ga, Ge, Pb, In, and Sb are close to that of Sn, suggesting the high possibility of doping those different elements in SnS_2. It has been reported that Al and Sr can be doped in SnS_2 by a simple soft chemical route.[29,30] Therefore, it is expected that Si, Be, Ca, Ba, Ga, Ge Pb, In and Sb can be verified experimentally in future.

Figure 2(b) shows the binding energies for non-metal doped SnS_2. Taking the binding energy of S doping as a reference, we can claim that B, C, O and F are easy to be doped in SnS_2. The C doped SnS_2 has been fabricated by using hydrothermal method and demonstrated as a high-efficient solar fuel catalyst under visible light.[31] Because Se and Te can also replace S in SnS_2,[23] we can estimate that N, Se, and Cl are possible to be doped in SnS_2 from the binding energy shown in Fig. 2(c). However, there are few reports regarding B, O, N, and Cl doping in SnS_2.

Figure 2(c) shows the binding energy of transition metal doped in SnS_2. Take the binding energy of Sn as a reference, we can find that Sc, Y, Lu, Ti, Zr, Hf, V, Nb, Ta, Cr, Mo, W, Mn, Tc, Re, Fe, Ru, Os, Co, Rh, Ir, Ni and Pt can be doped in SnS_2. Ni, Co and Mn doped SnS_2 have been synthesized by solvothermal method and can be applied for supercapacitors.[32] Fe, Cr and Y doped SnS_2 have also been successfully prepared by thermolysis method.[31,33] V and W doped SnS_2 have been demonstrated by spray pyrolysis technique.[34] Therefore, our prediction is consistent with previous experimental work.

Figure 3(a) shows the spin polarized DOS of pristine monolayer SnS_2. The band gap is 1.487 eV according to DFT calculation. Si has same valence electrons as Sn, and therefore, Si_{Sn} is isovalent doping, which will induce band gap change without defect states. The DOS shown in Fig. 3(b) confirms this assumption and Si_{Sn} will induce the change of band gap (1.367 eV). Because Al atom has one less electron than Sn atom, it is expected a p-type doping for Al substitution. From the DOS shown in Fig. 3(b), we can clearly observe the Fermi level cross the band edge states of the valence band, which is the signature of p-type doping. We expect Sb_{Sn} defect will induce n-type doping because Sb has one more valence electron than Sn. However, the defect states locate in the middle of the band gap and the Fermi level is far from the conduction band or valence band edge as shown in Fig. 3(d). Therefore, Sb_{Sn} defect will introduce trap states in SnS_2, which is consistent with previous experimental and theoretical results.[35,36]

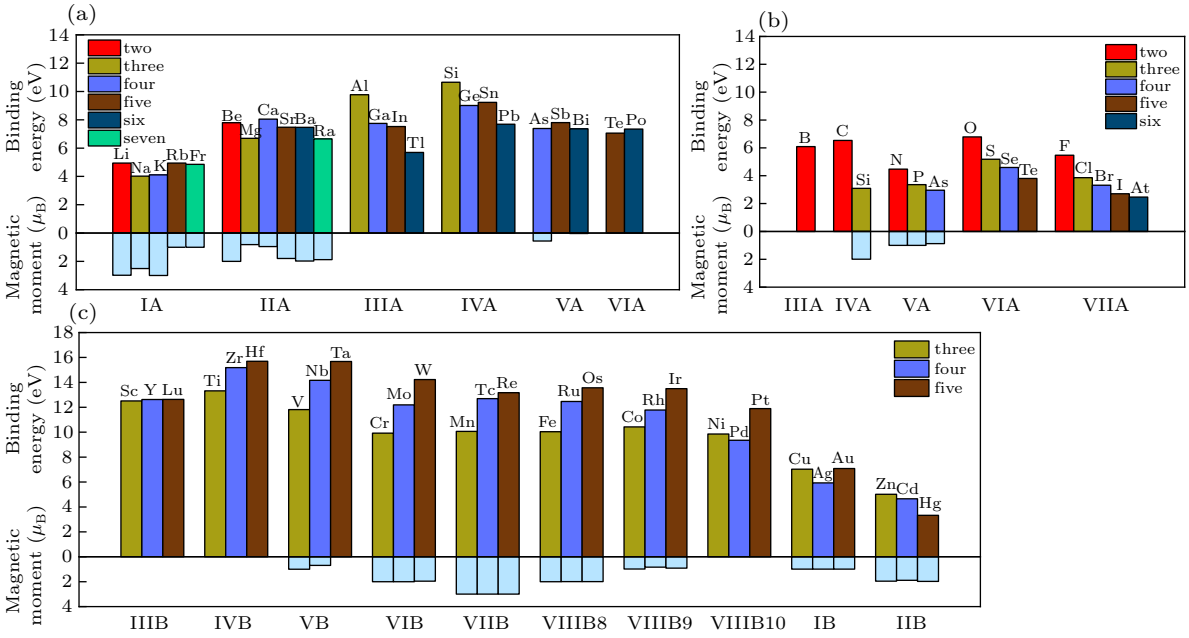


Fig. 2. Binding energies and magnetic moments of monolayer SnS_2 doped by (a) group A metal atoms from the period IA to VIA, (b) nonmetal from IIIA to VIIA, (c) group B metal atoms from IB to VIIIB.

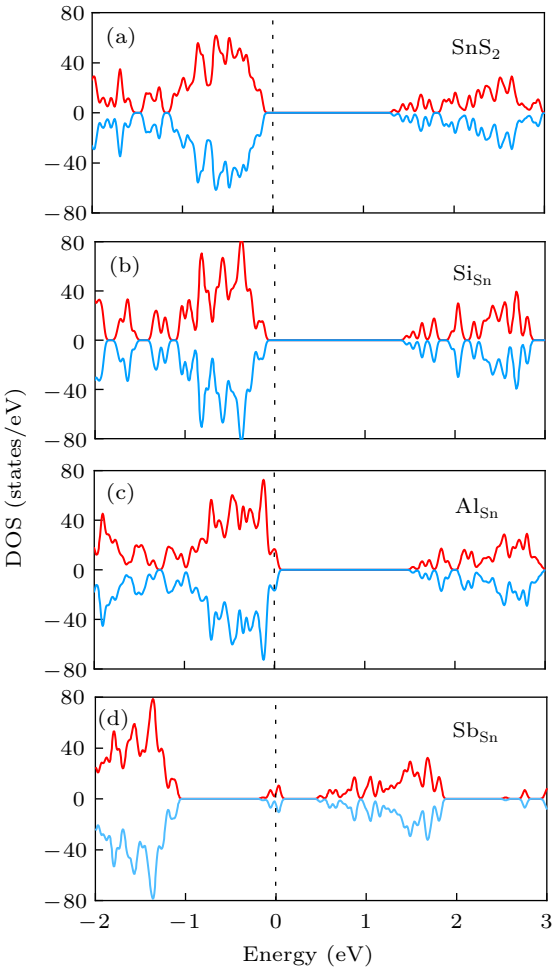


Fig. 3. Spin polarized density of states of (a) pristine, (b) Si_{Sn}, (c) Al_{Sn}, and (d) Sb_{Sn} doped monolayer SnS_2.

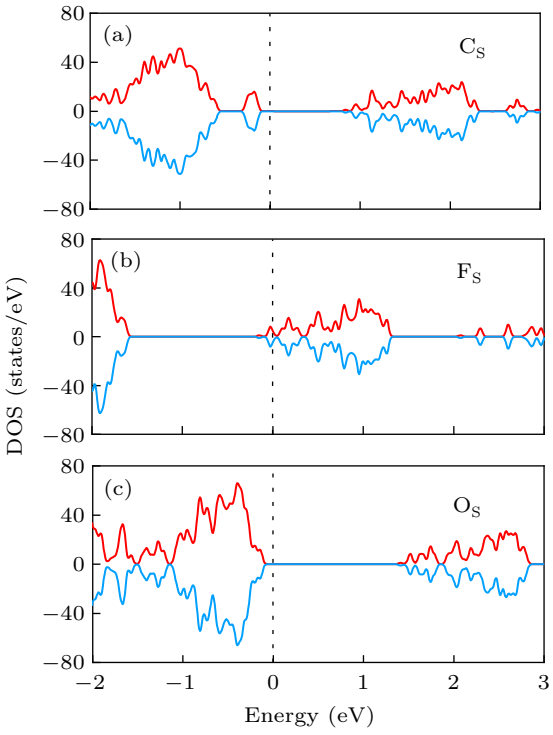


Fig. 4. Spin polarized density of states of (a) C_S, (b) F_S, and (c) O_S doped monolayer SnS_2.

Figure 4(a) shows the DOS for SnS_2 with C_S defect. There is an occupied defect state above the valence band edge, indicating the p-type doping of C_S. In contrast, F_S defect leads to a defect state close to the conduction band edge, indicating a n-type doping scenario, as shown in Fig. 4(b). As a typical isovalent doping, O_S leads to the change of band gap (1.454 eV) without defect states in the band gap as shown in Fig. 4(c). Similarly, Se_S and Te_S also induce change of band gap without defect states.

The valence state of transition metal ranges from +2 to +5. Therefore, it is also expecting p-type and n-type doping by transition metals substitution. Figure 5(a) shows the band

structure of Hf doped SnS_2, which evidently shows there is no defect state in the band gap. The absence of defect state can be attributed to the same valent state of Hf as that of Sn in SnS_2. In addition, both HfS_2 and monolayer SnS_2 are in the same space group and the in-plane lattice parameters for each compound are similar. Because of the band gap of monolayer HfS_2 is smaller than that of SnS_2, the doping of Hf in SnS_2 will reduce the band gap of SnS_2. The band gap of Hf doped SnS_2 with doping concentration of 6.25% is 1.228 eV, which is smaller than that of pristine SnS_2. We also can find that Zr, Pt, Pd, and Ni have the similar effect to Hf. The DOS for Sc_{Sn} in Fig. 5(b) shows that the Fermi level is on the valence band edge, indicating a p-type doping nature. Y_{Sn} and Lu_{Sn} have the same scenario.

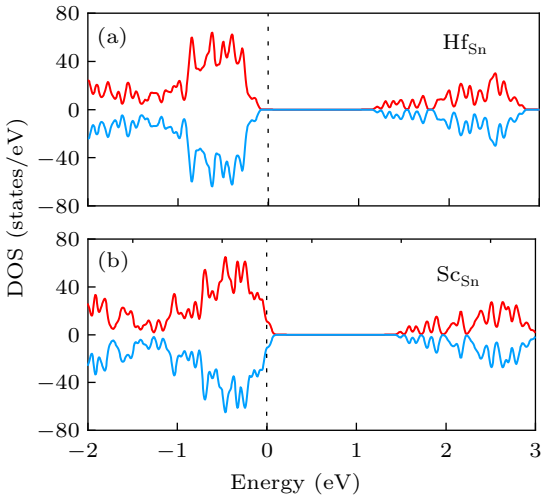


Fig. 5. Spin polarized density of states of (a) Hf_{Sn}, and (b) Sc_{Sn}, doped monolayer SnS_2.

For non-metal doping, the dopant with high binding energy is absent of magnetic moment. There are some dopants with non-zero magnetic moment, such as N_S, P_S and As_S. However, the binding energies for those dopants are low, indicating difficulty of formation. For dopant from IA group, the binding energy is low though magnetism is introduced by Li, Na, K doping. The introduction of magnetism by elements in IA group is consistent with previous calculation.[24] For dopant in IIA group, the formation energies are larger than that in IA group. The magnetic moments for those dopants range from 1.0 μ_B to 2.0 μ_B. Figure 6(a) shows the DOS of monolayer SnS_2 with Ca_{Sn} defect. The spin up and spin down DOS are unsymmetrical, indicating that Ca doping possibly leads to magnetism in SnS_2. Moreover, the Fermi level crosses the valence band edge, suggesting p-type doping.

For transition metal doping, the dopant from VIB, VIIB, VIIIB8 or VIIIB9 groups is with local magnetic moment and has high binding energies. The magnetic moments are around 2.0 μ_B, 3.0 μ_B, 2.0 μ_B and 1.0 μ_B for single dopant from VIB, VIIB, VIIIB8 and VIIIB9 groups, respectively. Magnetism has been predicted/observed in 2D transition metal doped monolayer 2D semiconductors, such as Mn doped MoS_2,[37] Fe doped SnS_2.[16] Figure 6(b) shows the spin polarized DOS of Mn doped SnS_2. Though Re and Mn are in the same group and magnetic moments both are ~ 3.0 μ_B, the spin polarized DOS of Re doped SnS_2 shown in Fig. 6(c) is quite different from that of Mn doped SnS_2. There are two more gap states in the spin up channel for Re doped SnS_2. V and Nb in VB group also introduce magnetism in SnS_2, while the magnetism is absent in Ta doped SnS_2. Therefore, the doping scenarios are different from elements in the same group.

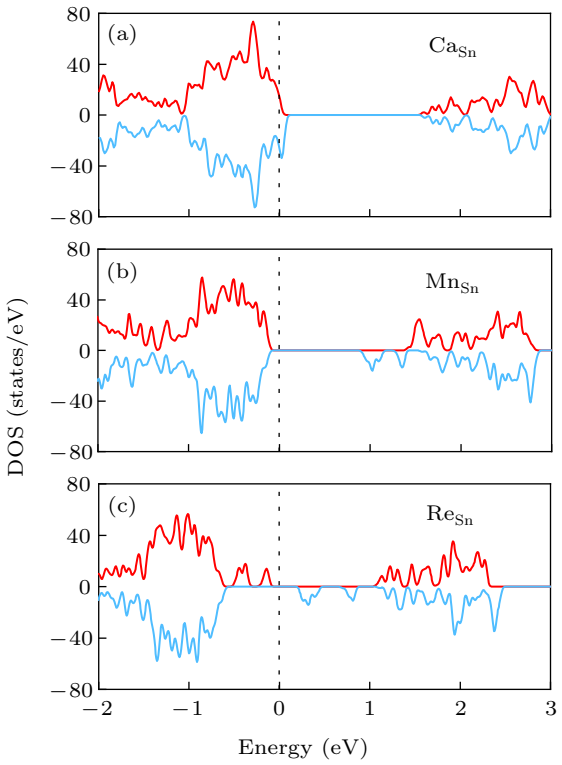


Fig. 6. Spin polarized density of states of (a) Ca_{Sn}, (b) Mn_{Sn}, and (c) Re_{Sn} doped monolayer SnS_2.

Due to valence state of each element is different from each other, the doping scenarios, including binding energy, electronic and magnetic properties, are different. Doping a specific element in SnS_2 depends on various factors, such as growth temperature, type of reactant, and abundance of reactant. In our present work, the calculated binding energy is applied to check the possibility of doping foreign element. To further verify the possibility of doping, the formation energy for doping on chemical potential should be investigated. However, it has been proven efficient and validity of evaluating the doping possibility by using the binding energy.[18,22,24,37] Some predictions by using such method have been experimentally verified, such as Fe, Co, and Mn doping in MoS_2.[38–40] By evaluating the binding energy shown in Fig. 2 and the carrier type for different element doping shown in Figs. 3 and 4, and Figs. S1–S6 in supporting information, we conclude

that C_S, Al_{Sn}, Sc_{Sn}, Lu_{Sn}, and Y_{Sn} are promising experimentally realized for p-type doping, as well as F_S, Sb_{Sn} and Ta_{Sn} for n-type doping without magnetism. In addition, we screen out some foreign elements doping that may introduce magnetism in SnS_2. Under doping concentration of 6.25%, the ferromagnetic state is 0.60 meV, 2598.95 meV, 637.75 meV, and 906.58 meV lower than non-magentic or antimagnetic state for Ca, Mn, Re, and Fe substitutional doping, respectively, see Table S1 in supporting information. The Curie temperature (T_C) is an important parameter of a ferromagnetic semiconductor. Based on the mean-field theory and Heisenberg model we estimate T_C using the relation $k_B T_C = (2/3)\Delta E$,[41,42] where k_B and ΔE are the Boltzmann constant and the energy difference of ferromagnetic and non-magnetic/antiferromagnetic states, respectively. The estimated values of T_C are listed in Table S1, together with magnetic moments. The T_C of Re_{Sn} is around 30 K, while others are lower than 10 K. It is well known that doping concentration also affect magnetic coupling and the value of T_C. We take Re and Fe doped SnS_2 as two representatives. The two Re ions are antiferromagnetic coupled, while Fe ions remains ferromagnetic coupled for doping concentration of 12.5%. The detailed magnetic ground state and further exploration of high T_C of a certain doping should be investigated in future.

4. Conclusion

By using high throughput first-principles calculation, we comprehensively investigate the substitutional doping in monolayer SnS_2. Metal dopants from group A can induce p-type doping (Al_{Sn}), deep states in the gap (Sb_{Sn}), or band gap change without defect states (Si_{Sn}). However, metal dopants from group A can not introduce n-type doping from our calculations. Nonmetal dopants from group A not only can introduce n-type doping (F_S), p-type doping (C_S), and band gap variation (O_S). Transition metal dopants from VB to VIIIB9 can introduce magnetism in SnS_2 and high binding energy for each dopant indicates high possibility of growth transition metal doped SnS_2. Our present work provides a comprehensive view of chemical doping effect on carrier and magnetism of SnS_2, which is important for field effect transistor, optoelectronic device and spintronics.

References

[1] Xia C, Peng Y, Zhang H, Wang T, Wei S and Jia Y 2014 *Phys. Chem. Chem. Phys.* **16** 19674
[2] Huang Y, Sutter E, Sadowski J T, Cotlet M, Monti O L A, Racke D A, Neupane M R, Wickramaratne D, Lake R K, Parkinson B A and Sutter P 2014 *ACS Nano* **8** 10743
[3] Sun Y F, Cheng H, Gao S, Sun Z H, Liu Q H, Liu Q, Lei F C, Yao T, He J F, Wei S Q and Xie Y 2012 *Angew. Chem., Int. Ed.* **51** 8727
[4] Chen X, Hou Y, Zhang B, Yang X H and Yang H G 2013 *Chem. Commun.* **49** 5793
[5] Xu L, Zhang P, Jiang H, Wang X, Chen F, Hu Z, Gong Y, Shang L, Zhang J, Jiang K and Chu J 2019 *Small* **15** 1904116
[6] Seo J, Jang J, Park S, Kim C, Park B and Cheon J 2008 *Adv. Mater.* **20** 4269
[7] Wang D, Tang M, Jiang H, Li M, Jiang S, Sun L and Sun J 2020 *Chem. Eng. J.* **400** 125814
[8] Du W, Deng D, Han Z, Xiao W, Bian C and Qian X 2011 *Cryst. Eng. Comm.* **13** 2071
[9] Li Y, Tang L B, Li R J, Xiang J Z, Teng K S and Lau S P 2019 *Chin. Phys. B* **28** 037801
[10] Sun L, Zhou W, Liu Y, Lu Y, Liang Y and Wu P 2017 *Comput. Mater. Sci.* **126** 52
[11] An X, Yu J C and Tang J 2014 *J. Mater. Chem. A* **2** 1000
[12] Liu X, He D, He J, Wang Y and Fu M 2019 *Chin. Phys. B* **28** 118101
[13] Chen G X, Fan X B, Li S Q and Zhang J M 2019 *Acta Phys. Sin.* **68** 237303 (in Chinese)
[14] Lin L, Guo Y P, He C Z, Tao H L, Huang J T, Yu W Y, Chen R X, Lou M S and Yan L B 2020 *Chin. Phys. B* **29** 097102
[15] Dietl T 2010 *Nat. Mater.* **9** 965
[16] Li B, Xing T, Zhong M Z, Huang L, Lei N, Zhang J, Li J B and Wei Z M 2017 *Nat. Commun.* **8** 1958
[17] Dietl T, Bonanni A and Ohno H 2019 *J. Semicond.* **40** 080301
[18] Luo M, Xu Y E and Song Y X 2018 *Comput. Mater. Sci.* **154** 309
[19] Yu D, Liu Y, Sun L, Wu P and Zhou W 2016 *Phys. Chem. Chem. Phys.* **18** 318
[20] Xia C, Zhao X, Peng Y, Zhang H, Wei S and Jia Y 2015 *Superlattices Microstruct.* **85** 664
[21] Ali A, Zhang J M, Muhammad I, Wei X M, Huang Y H, Rehman M U and Ahmad I 2020 *Thin Solid Films* **705** 138045
[22] Xiao W Z, Xiao G, Rong Q Y, Chen Q and Wang L L 2017 *J. Magn. Magn. Mater.* **438** 152
[23] Ullah H, Noor-A-Alam M and Shin Y H 2020 *J. Am. Ceram. Soc.* **103** 391
[24] Xiao W Z, Xiao G, Rong Q Y and Wang L L 2018 *Physica E* **99** 182
[25] Liu X Y, Wei D H and Zhao J H 2019 *J. Semicond.* **40** 080101
[26] Blochl P E 1994 *Phys. Rev. B* **50** 17953
[27] Perdew J P, Burke K and Ernzerhof M 1996 *Phys. Rev. Lett.* **77** 3865
[28] Kresse G and Furthmuller J 1996 *Phys. Rev. B* **54** 11169
[29] Prabha D, Ilangovan S, Balamurugan S, Suganya M, Anitha S, Nagarethinam V S and Balu A R 2017 *Optik* **142** 301
[30] Prabha D, Ilangovan S, Srivind J, Suganya M, Anitha S, Balamurugan S and Balu A R 2017 *J. Mater. Sci.: Mater. Electron.* **28** 15556
[31] Shown I, Samireddi S, Chang Y C, Putikam R, Chang P H, Sabbah A, Fu F Y, Chen W F, Wu C I, Yu T Y, Chung P W, Lin M C, Chen L C and Chen K H 2018 *Nat. Commun.* **9** 169
[32] Chu H, Zhang F, Pei L, Cui Z, Shen J and Ye M 2018 *J. Alloys Compd.* **767** 583
[33] Heiba Z K, Mohamed M B and Abdel Kader M H 2018 *J. Electron. Mater.* **47** 2945
[34] Yassin O A, Abdelaziz A A and Jaber A Y 2015 *Mater. Sci. Semicond. Process.* **38** 81
[35] Liu J, Liu X, Chen Z, Miao L, Liu X, Li B, Tang L, Chen K, Liu Y, Li J, Wei Z and Duan X 2018 *Nano Res.* **12** 463
[36] Xue Y, Zhou W, Ding L, Jiang J, Ning H, Liang X, Zhou W, Guo J and Huang D 2020 *Phys. Lett. A* **384** 126695
[37] Cheng Y C, Zhu Z Y, Mi W B, Guo Z B and Schwingenschlogl U 2013 *Phys. Rev. B* **87** 100401
[38] Li B, Huang L, Zhong M Z, Huo N J, Li Y T, Yang S X, Fan C, Yang J H, Hu W P, Wei Z M and Li J B 2015 *Acs Nano* **9** 1257
[39] Li Q, Zhao X X, Deng L J, Shi Z T, Liu S, Wei Q L, Zhang L B, Cheng Y C, Zhang L, Lu H P, Gao W B, Huang W, Qiu C W, Xiang G, Pennycook S J, Xiong Q H, Loh K P and Peng B 2020 *Acs Nano* **14** 4636
[40] Duan H L, Guo P, Wang C, Tan H, Hu W, Yan W S, Ma C, Cai L, Song L, Zhang W H, Sun Z H, Wang L J, Zhao W B, Yin Y W, Li X G and Wei S Q 2019 *Nat. Commun.* **10** 1584
[41] Kudrnovský J, Turek I, Drchal V, Máca F, Weinberger P and Bruno P 2004 *Phys. Rev. B* **69** 115208
[42] Máca F, Kudrnovský J, Drchal V and Bouzerar G 2008 *Appl. Phys. Lett.* **92** 212503